JOURNAL OF MATERIALS SCIENCE 26 (1991) 4427–4432

Transport characteristics related with microstructure of (Bi, Pb)–Sr–Ca–Cu–O superconductor prepared by the sol–gel method

AKIYOSHI NOZUE, HIROYUKI NASU, KANICHI KAMIYA
Department of Industrial Chemistry, Faculty of Engineering, Mie University, Kamihama-cho, Tsu-shi 514, Japan

KATSUHISA TANAKA
Department of Industrial Chemistry, Faculty of Engineering, Kyoto University, Yoshida-honmachi, Sakyo-ku, Kyoto-shi 606, Japan

Differences in the transport characteristics of $Bi_2Sr_2Ca_2Cu_3O_y$ (high-T_c phase) superconducting ceramics produced by two-step heat-treatment (calcination and reheating at various temperatures) of metal acetate-derived gels are discussed in relation to their microstructure. Variation of the volume fraction increase rate of the high-T_c phase, which depends on the calcination temperature, results in much difference in the transport characteristics of the resultant samples. Superconducting bodies possessing a higher $T_{c(end)}$ and critical current density can be obtained at a lower volume fraction increase-rate of the high-T_c phase. It is considered that the origin of the above results is an improvement of the weak-link structure.

1. Introduction

In the Bi–Sr–Ca–Cu–O system, it is known that there exist two superconducting phases with the composition of $Bi_2Sr_2CaCu_2O_x$ (low-T_c phase) and $Bi_2Sr_2Ca_2Cu_3O_y$ (high-T_c phase) [1]. It is also known that the high-T_c phase is formed via formation of the low-T_c phase [2]. The partial substitution of Pb for Bi and addition of excess Ca and/or Cu to the stoichiometric composition of the high-T_c phase has been found to facilitate the formation of the pure high-T_c phase [3–5]. We have previously reported that the process in which the metal acetate-derived gel was calcined at the nucleation temperature of the high-T_c phase and reheated at higher temperature was very effective for the formation of the high-T_c phase [6].

On the other hand, since the oxide superconductors are fabricated as polycrystalline ceramics in most cases, the superconducting properties are affected by their microstructure, which is much influenced by the processing [7, 8]. In particular, in the production of polycrystalline superconducting ceramics composed of the high-T_c phase, it has been reported that their transport characteristics are extremely influenced by several factors, such as sintering conditions [9, 10] and starting composition [11, 12]. Furthermore, it has been shown in our previous study that their transport characteristics are also much affected by the calcination temperature, even under the same reheating conditions [13]. However, the origin of the above phenomenon has not been clarified, although the verification of the origin would give us important information for obtaining superconducting ceramics composed of the high-T_c phase with a higher transport current density.

In the present study, in order to clarify the differences in the transport characteristics of $Bi_2Sr_2Ca_2Cu_3O_y$ superconducting ceramics produced by the sol–gel method under different heat-treatment conditions, several experiments were conducted.

2. Experimental procedure

2.1. Preparation of samples

The precursors for the superconductor were prepared by the sol–gel method. As starting reagents, $Bi(NO_3)_3 \cdot 5H_2O$, $Pb(CH_3COO)_2 \cdot 3H_2O$, $Sr(CH_3COO)_2 \cdot 0.5H_2O$, $Ca(CH_3COO)_2 \cdot H_2O$ and $Cu(CH_3COO)_2 \cdot H_2O$ were used. These reagents were weighed so that the molar ratios of Bi, Pb, Sr, Ca and Cu were equal to 0.91 : 0.17 : 0.96 : 1.0 : 1.5. They were dissolved in an aqueous solution of acetic acid and ammonia. The pH value of the solution was adjusted to 5.5. The solution became viscous on heating at 50–70 °C. By heating at 90 °C, the sol was set to a transparent wet gel. The details of the experimental procedure for preparation of the gel have been described elsewhere [14].

The resultant gel was firstly heat-treated at 250 °C for 5 h, and then calcined for 12 h in air at 740, 800, 830 or 845 °C with a heating rate of 100 °C h^{-1}. The specimens thus obtained were pulverized and pressed into pellets 1 cm in diameter and 1 mm in thickness, reheated at 845 °C for 6–48 h in air and cooled down to room temperature in the furnace.

2.2. Measurements

Identification of the crystals formed was carried out by means of powder X-ray diffraction analysis using

0022–2461/91 $03.00 + .12

nickel-filtered CuK_α radiation. The volume fraction of the high-T_c phase in the samples was evaluated from the relative intensity of the X-ray diffraction peaks, $I_{h(00\underline{12})}/(I_{h(00\underline{12})} + I_{l(115)})$, where I_h and I_l denote the diffraction intensities of the high- and low-T_c phases, respectively. Since the (00$\underline{12}$) peak of the high-T_c phase overlapped the (00$\underline{10}$) peak of the low-T_c phase, $I_{h(00\underline{12})}$, was evaluated by subtracting $I_{l(00\underline{10})}$ from the observed $I_{h(00\underline{12})}$ assuming that $I_{l(00\underline{10})}/I_{l(115)} = 0.36$ [15]. Lattice constants of the high-T_c phase were measured on the basis of d-values for (00$\underline{10}$), (200) and (00$\underline{14}$) lines calibrated by the Si(1 1 $\bar{1}$) line. In order to evaluate the degree of orientation of the high-T_c phase, X-ray diffraction was conducted for some sintered disc-shaped samples.

The microstructure was observed by a scanning electron microscope (SEM). Bulk density was measured with a pycnometer.

The resistivity measurements were performed at 50 to 300 K by using a four-probe method with an electrical current of 5 mA. Silver paste was used as electrodes. In order to evaluate the temperature dependence of critical current density, the measuring-current dependence of $T_{c(end)}$ was measured, and the critical current density at the resultant $T_{c(end)}$ was estimated by dividing the measuring current by the cross-sectional area of the measured sample between electrodes.

3. Results

3.1. Formation of the high-T_c phase

Fig. 1 shows the reheating-time dependence of the volume fraction of the high-T_c phase in samples calcined at various temperatures and reheated at 845 °C for 6 to 48 h. It is seen that the volume fraction of the high-T_c phase increases in the order of calcination temperature 740 < 800 < 845 < 830 °C. The major crystalline phases in the samples calcined at 740 and 800 °C are the very low-T_c phase and the low-T_c phase, respectively, and no high-T_c phase is observed. On reheating at 845 °C, the high-T_c phase is formed. However, for the sample calcined at 740 °C the volume fraction of the high-T_c phase is about 70% after reheating for 48 h. On the other hand, the samples calcined at 830 and 845 °C contain a small amount of the high-T_c phase which increases rapidly on subsequent reheating at 845 °C, especially for the sample calcined at 830 °C. This tendency comes from the fact that the nucleation of the high-T_c phase is likely to take place around 830 °C as described elsewhere [6].

3.2. Critical temperature (T_c)

Fig. 2 shows the reheating-time dependence of $T_{c(end)}$ for samples calcined at various temperatures. Fig. 3 shows the temperature dependence of resistivity for samples reheated at 845 °C for 48 h after calcination at various temperatures. For the samples calcined at 740 and 800 °C, $T_{c(end)}$ rises as the reheating time increases. On reheating for 48 h, the R–T curves become one-step and show $T_{c(end)}$ above 100 K. On the other hand, the sample calcined at 830 °C and

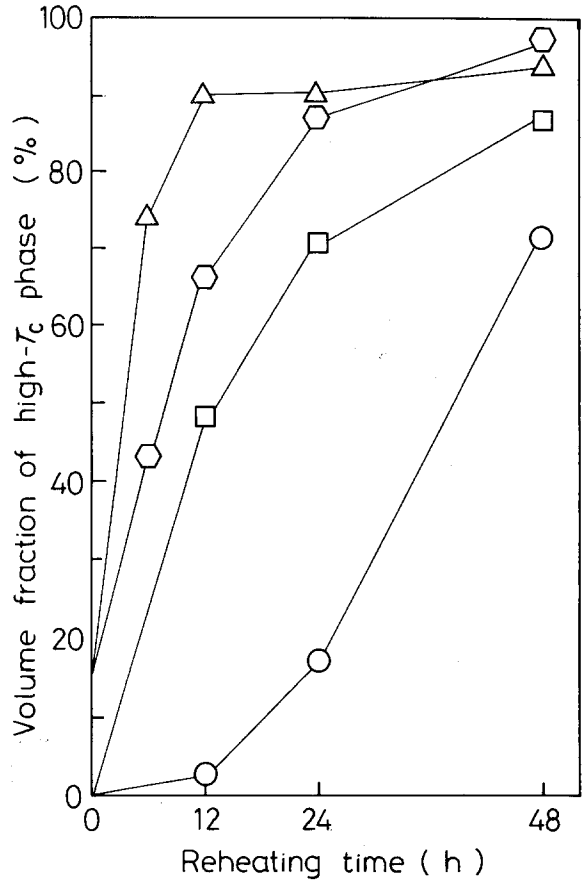

Figure 1 Reheating-time dependence of the volume fraction of the high-T_c phase, evaluated from the relative intensities of the X-ray diffraction peaks, after calcination at different temperatures: (○) 740 °C, (□) 800 °C, (△) 830 °C, (⬡) 845 °C.

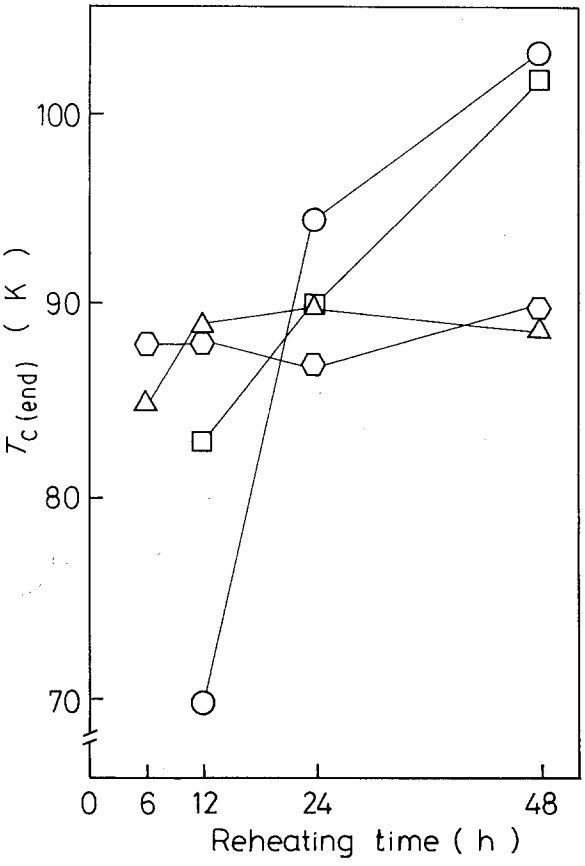

Figure 2 $T_{c(end)}$ of samples reheated at 845 °C after calcination at different temperatures: (○) 740 °C, (□) 800 °C, (△) 830 °C, (⬡) 845 °C.

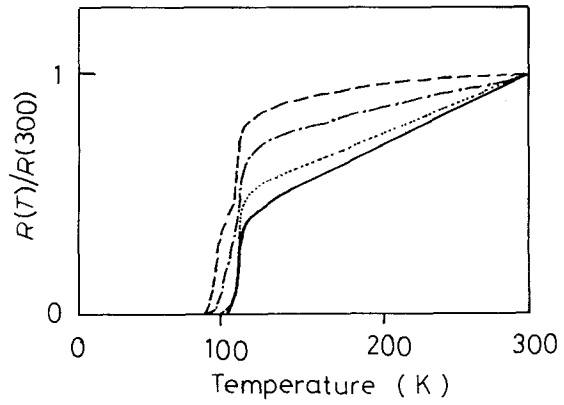

Figure 3 Temperature dependence of resistivity for samples reheated at 845 °C for 48 h after calcination at different temperatures: (——) 740 °C, (. . .) 800 °, (– –) 830 °C, (– · –) 845 °C.

reheated at 845 °C for 12 h shows a two-step R–T curve and $T_{c(end)}$ below 90 K, although the volume fraction of the high-T_c phase is more than 90%. Reheating for 48 h results in similar R–T behaviour to the above. Moreover, for the samples calcined at 845 °C the same trend is observed. All the samples show $T_{c(onset)}$ around 110 K.

3.3. Lattice constants

Lattice constants of the high-T_c phase in samples reheated at 845 °C for 48 h after calcination at 740, 800, 830 and 845 °C are listed in Table I. It is seen that

TABLE I Lattice constants of the high-T_c phase in samples reheated at 845 °C for 48 h after calcination at the indicated temperature

Calcination temperature (°C)	a-axis(nm)	c-axis(nm)
740	0.5416	3.712
800	0.5413	3.716
830	0.5414	3.714
845	0.5414	3.712

both a-axis and c-axis show no variation with the calcination temperature.

3.4. SEM observations

Fig. 4a to d depicts SEM photographs of fractured surface of the samples reheated at 845 °C for 48 h after calcination at 740, 800, 830 and 845 °C, respectively. Almost all of the samples are composed of plate-like crystals which seem at first glance to be irregularly oriented. X-ray diffraction patterns of the disc-shape samples are shown in Fig. 5. Since the (0 0 l) lines of the high-T_c phase are a little stronger than the others, the grains in all samples seem to be slightly oriented with respect to the c-axis, perpendicular to the specimen surface. The degree of orientation of the high-T_c grains is almost the same in all samples.

Here, the grain size of the high-T_c phase in each

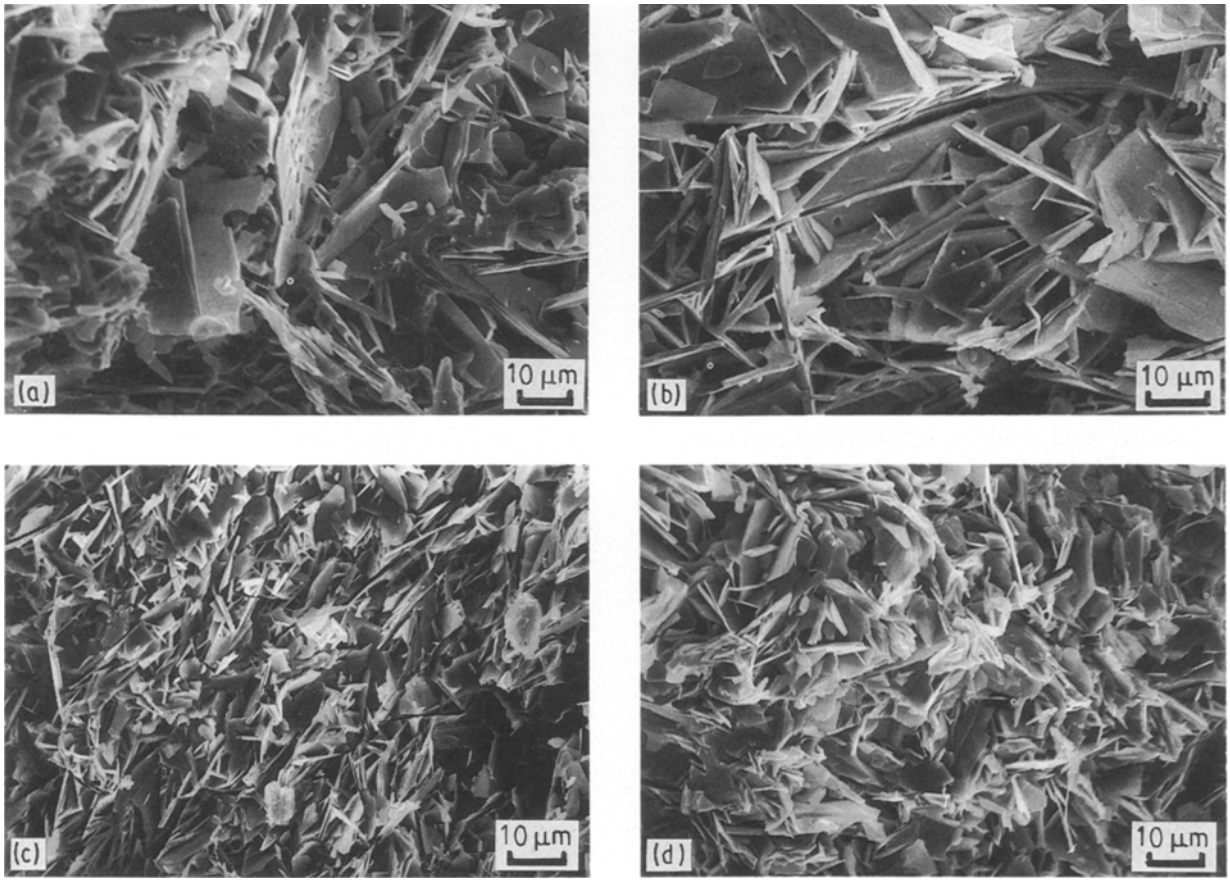

Figure 4 SEM photographs of the fractured surface of samples reheated at 845 °C for 48 h after calcination at (a) 740 °C, (b) 800 °C, (c) 830 °C, (d) 845 °C.

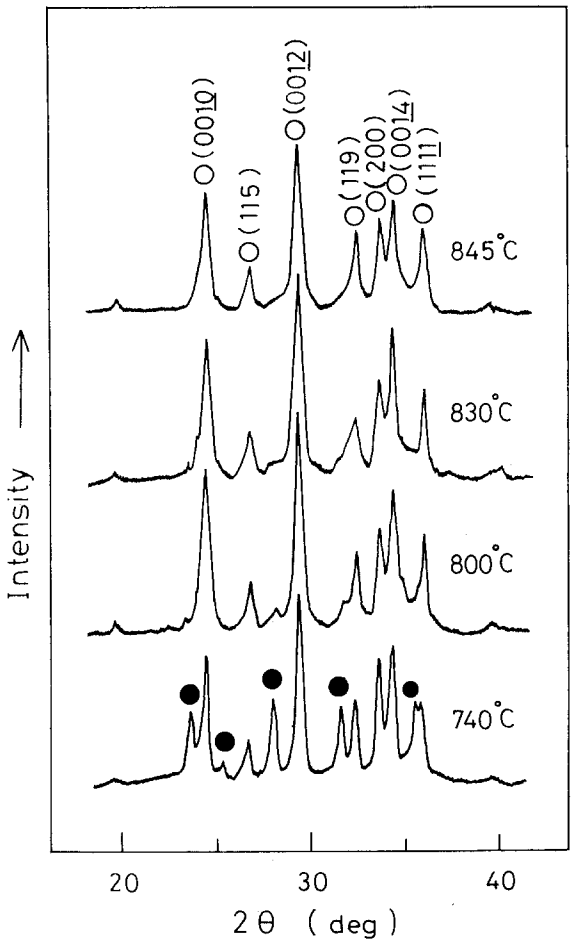

Figure 5 X-ray diffraction patterns of disc-shaped samples reheated at 845 °C for 48 h after calcination at the indicated temperatures: (○) high-T_c, (●) low-T_c phase.

sample is worthy of notice. The grain size of the high-T_c phase increases in the order of calcination temperature 830 < 845 < 800 < 740 °C. In particular, in the samples reheated at 845 °C for 48 h after calcination at 740 or 800 °C, the grain size of the high-T_c phase is fairly large compared with the others.

3.5. Bulk density of the samples

Results for the bulk density of samples reheated at 845 °C for 48 h after calcination at 740, 800, 830 and 845 °C are listed in Table II. Bulk densities of the samples reheated at 845 °C for 48 h after calcination at 830 or 845 °C, which have smaller grains, are slightly higher than those of samples with larger grains. However, the densities of the samples prepared in the present study are considerably lower than the theoretical value, 6.55 g cm^{-3} [16].

3.6. Temperature dependence of critical current density

In order to obtain information on Josephson weak links, the temperature dependence of critical current density was examined. It is known that the critical current density depends on temperature as $[1 - (T/T_c)]$ for an SIS junction, whereas for an SNS junction it varies as $[1 - (T/T_c)]^2$ near the critical temperature [17]. Here, S, I and N denote superconductor, insulator and metal, respectively. Fig. 6 shows the relation between $[1 - (T/T_c)]$ and critical current density, and Fig. 7 shows plots of $[1 - (T/T_c)]^2$ versus J_c near the critical temperature (108 K). As seen in Figs 6 and 7, the critical current density for all samples depends on the temperature not as $[1 - (T/T_c)]$ but as $[1 - (T/T_c)]^2$. The slope becomes larger in the order of calcination temperature 830 < 845 < 800 < 740 °C. In particular, the slope for the samples reheated at 845 °C for 48 h after calcination at 740 and 800 °C is considerably larger than the others.

TABLE II Bulk density of samples reheated at 845 °C for 48 h after calcination at the indicated temperature

Calcination temperature (°C)	Bulk density (g cm^{-3})
740	4.0
800	3.8
830	4.3
845	4.1
Theoretical value	6.55

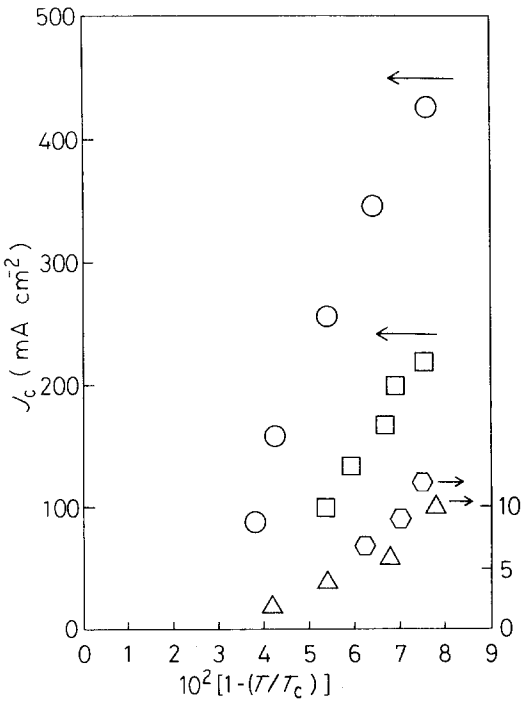

Figure 6 $[1 - (T/T_c)]$ versus J_c plots for samples reheated at 845 °C for 48 h after calcination at different temperatures: (○) 740 °C, (□) 800 °C, (△) 830 °C, (⬡) 845 °C.

4. Discussion

As can be seen in Fig. 1, calcination around 830 °C is most effective for the preferential formation of the high-T_c phase upon reheating at a higher temperature. However, the sample calcined at 830 °C and reheated at 845 °C for 12 h shows a two-step R–T curve and $T_{c(end)}$ at 89 K, although the volume fraction of the high-T_c phase is more than 90%. Reheating for 48 h results in similar R–T behaviour to the above. Moreover, for the samples calcined at 845 °C the same trend is observed.

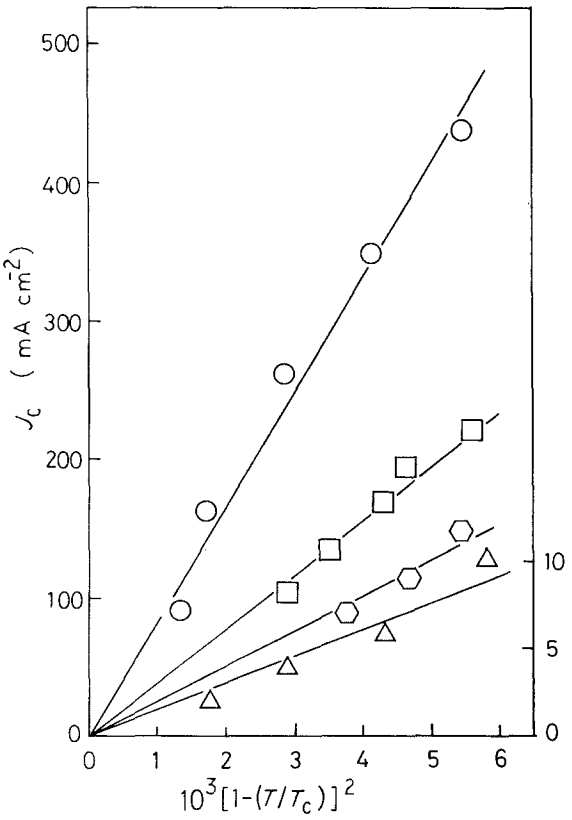

Figure 7 $[1-(T/T_c)]^2$ versus J_c plots for samples reheated at 845 °C for 48 h after calcination at different temperatures: (○) 740 °C, (□) 800 °C, (△) 830 °C, (⬡) 845 °C.

On the other hand, calcination at 740 or 800 °C makes the formation of the high-T_c phase difficult upon reheating, but $T_{c(end)}$ above 100 K can be attained by reheating at 845 °C for 48 h. It is seen in Figs 1 and 2 that superconducting bodies possessing a higher $T_{c(end)}$ can be obtained at a lower volume fraction increase-rate of the high-T_c phase, which results from suppressed nucleation of the high-T_c phase.

Here, it is reasonable to state that the differences in $T_{c(end)}$ are attributed to variation of transport characteristics among samples. In the following, the reason for the different transport characteristics among samples reheated at 845 °C for 48 h after calcination at 740, 800, 830 and 845 °C will be discussed.

It has been considered that, in the polycrystalline oxide superconducting ceramics, intergranular rather than intragranular current is associated with degradation of the transport critical current density [18]. As can be seen in Table I, the lattice constants of the present samples are hardly affected by the calcination temperature, and have no correlation with the volume fraction increase-rate of the high-T_c phase. Furthermore, from Fig. 3 it is seen that all samples show $T_{c(onset)}$ around 110 K regardless of the volume fraction increase-rate of the high-T_c phase. It is therefore concluded that in the present case as well, intergranular current seems to control the transport characteristics of all samples.

As possible causes of degradation of the transport current density, low bulk density, microcracking, irregular orientation of the grains with intrinsic anisotropy of the superconducting properties, and Josephson weak links have been listed [19, 20].

As can be seen in Table II, all samples have a low bulk density which is considerably lower than the theoretical value. The bulk densities of samples with a higher $T_{c(end)}$ are slightly lower than the others. Further, it is seen from Fig. 5 that the degree of orientation of the high-T_c grains is almost the same in all samples. These results indicate that the differences of transport characteristics among the samples are not ascribed to low bulk density and the orientation of high-T_c grains.

Many investigators have reported that the size of the superconducting grains in the Y–Ba–Cu–O system influences the transport critical current density [21, 22]. In that system, the transport critical current density tends to increase at small grain size, because the degree of microcracking can be diminished by decreasing the grain size. In the present study, however, the samples with larger grains, in which microcracking may tend to be generated, show a higher transport critical current density than those with smaller grains. From these facts, it is considered that microcracking due to a large grain size cannot be a dominant factor for determining the transport characteristics of the samples obtained in the present study.

Consequently, it can be said that the Josephson weak-link structures of each sample greatly influence the transport characteristics of the present samples. The presence of Josephson weak links is confirmed by the strong field dependence of transport critical current density, as has been reported for polycrystalline superconducting ceramics [7]. Considering the bulk polycrystalline superconductors as multi-circuits of Josephson junctions, their transport critical current density should be independent of grain size. That is, the effects of multiple Josephson junctions are not additive, and additional grain boundaries along the current percolation path do not further diminish the transport critical current density. Roshko *et al.* [23] have investigated the grain-size effect on the transport critical current density for $La_{2-x}Sr_xCuO_4$ with uniform equiaxed microstructure, and concluded that a variation of grain size has no significant effect on the transport critical current density when the transport current is controlled by weak-links at grain boundaries.

In order to examine the Josephson weak-link properties of the samples at a grain boundary, it is important to measure the temperature dependence of the critical current density near the critical temperature. This measurement has been conducted for the polycrystalline superconducting ceramics by several investigators [24, 25]. It is well known that the critical current density depends on the temperature as $[1-(T/T_c)]$ for an SIS junction, whereas for an SNS junction it varies as $[1-(T/T_c)]^2$ near the critical temperature [17]. In Figs 6 and 7 it is observed that the critical current density for all the present samples depends on the temperature not as $[1-(T/T_c)]$ but as $[1-(T/T_c)]^2$. These results suggest that the barrier in the grain boundary junctions in all samples is metallic. The behaviour of an SNS junction follows the follow-

ing equation near the critical temperature [26]:

$$J_c(T) = A\left(\frac{T_c - T}{T_c}\right)^2 \exp\left(-\frac{2d_N}{\xi_N}\right) \quad (1)$$

Here, for a general SNS junction, $2d_N$ is the thickness of the normal layer (metal), ξ_N is the length of electron-pair diffusion into the normal layer and A is a constant which depends on the materials of the S and N layers and the quality of the S–N interface. In Fig. 7, the slope of each line corresponds to the product of A and $\exp(-2d_N/\xi_N)$. For polycrystalline superconducting ceramics, $2d_N$ may correspond to the thickness of the grain boundary, and if the properties of the high-T_c phase are the same in all samples, A and ξ_N depend on the composition of the grain boundary and/or the quality of the superconductor–grain boundary interface. It can be seen from the plot of $[1 - (T/T_c)]^2$ versus J_c that when the volume fraction increase-rate of the high-T_c phase is low, the slope becomes larger. In particular, reduction of the nucleation of the high-T_c phase during calcination seems to result in a larger slope, that is, the slope for the sample calcined at 740 °C is about 50 times larger than that for the sample calcined at 830 °C. According to Equation 1, these results imply that the formation of the high-T_c phase formed at reduced nucleation and lower volume fraction increase-rate leads to fairly thin grain boundaries, and/or much improvement of the composition of the grain boundary and/or the quality of the superconductor–grain boundary interface.

5. Conclusion

In order to verify the differences in transport current behaviour for $Bi_2Sr_2Ca_2Cu_3O_y$ superconducting ceramics produced by two-step heat-treatment of the metal acetate-derived gels, i.e. calcination and reheating, several experiments were conducted. In the production of a polycrystalline superconductor composed of the high-T_c phase, it was clarified that variation of the volume fraction increase-rate of the high-T_c phase, which depends on the calcination temperature, results in a different Josephson weak-link structure in the resultant samples. It was found that the formation of a high-T_c phase with reduced nucleation and a lower volume fraction increase-rate improves the weak-link structure and makes the transport critical current density higher.

Acknowledgement

The authors would like to thank Professor O. Yamamoto and Professor Y. Takeda of the Department of Chemistry for Materials, Mie University, for the electrical measurements and SEM observations.

References

1. H. MAEDA, Y. TANAKA, M. FUKUTOMI and T. ASANO, *Jpn. J. Appl. Phys.* **27** (1988) L209.
2. N. KIJIMA, H. ENDO, J. TSUCHIYA, A. SUMIYAMA, M. MIZUNO and Y. OGURI, *ibid.* **27** (1988) L1852.
3. M. TAKANO, J. TAKADA, K. ODA, H. KITAGUCHI, Y. MIURA, Y. IKEDA, Y. TOMII and H. MAZAKI, *ibid.* **27** (1988) L1041.
4. N. KIJIMA, H. ENDO, J. TSUCHIYA, A. SUMIYAMA, M. MIZUNO and Y. OGURI, *ibid.* **27** (1988) L821.
5. U. ENDO, S. KOYAMA and T. KAWAI, *ibid.* **27** (1988) L1476.
6. K. TANAKA, A. NOZUE and K. KAMIYA, *ibid.* **28** (1989) L934.
7. J. W. EKIN, *Adv. Ceram. Mater.* **2** (1987) 586.
8. D. DIMOS, P. CHANDHARI, J. MANNHART and F. K. LeGOUES, *Phys. Rev. Lett.* **61** (1988) 219.
9. A. OOTA, K. OHBA, A. ISHIDA, A. KIRIHIGASHI, K. IWASAKI and H. KUWAJIMA, *Jpn. J. Appl. Phys.* **28** (1989) L1171.
10. T. WADA, N. SUZUKI, A. MAEDA, S. UCHIDA, K. UCHINOKURA and S. TANAKA, *ibid.* **27** (1988) L1031.
11. M. MIZUNO, H. ENDO, J. TSUCHIYA, N. KIJIMA, A. SUMIYAMA and Y. OGURI, *ibid.* **27** (1988) L1225.
12. R. RAMESH, S. M. GREEN, YU MEI, A. E. MANZI and L. LUO, *J. Appl. Phys.* **66** (1989) 1265.
13. A. NOZUE, H. NASU, K. TANAKA and K. KAMIYA, *Jpn. J. Appl. Phys.* **28** (1989) L2161.
14. K. TANAKA, A. NOZUE and K. KAMIYA, *J. Mater. Sci.* **25** (1990) 3551.
15. M. ONODA, A. YAMAMOTO, E. TAKAYAMA-MUROMACHI and S. KANEKAWA, *Jpn. J. Appl. Phys.* **27** (1988) L833.
16. E. TAKAYAMA-MUROMACHI, Y. UCHIDA, A. ONO, F. IZUMI, M. ONODA, Y. MATSUI, K. KOSUDA, S. TAKEKAWA and K. KATO, *ibid.* **27** (1988) L365.
17. A. BARONE and G. PATERNO, "Physics and Applications of the Josephson Effect" (Wiley, 1984) p. 164.
18. E. YAMAGA, K. TACHIKAWA and N. ICHINOSE (eds), "Koon-Chodendou-Nyumon" (Ohm-sha, Tokyo, 1989).
19. J. W. EIKIN, A. I. BRAGINSKI, A. J. PANSON, M. A. JANOCKO, D. W. CAPONE, N. J. ZALUZEU, B. FLANDERMEYER, O. F. de LIMA, M. HONG, J. KWO and H. LIOU, *J. Appl. Phys.* **62** (1987) 4821.
20. D. C. LARBALESTIER, D. MAEUMLING, X. CAI, J. SEUNTJENS, T. WILLIS, J. McKINNEL, D. HAMPSHIRE, P. LEE, C. MEINGAST, H. MULLER, R. D. RAY, R. G. DILLENBURY, E. E. HELLSTROM and R. JOYNT, *ibid.* **62** (1987) 3308.
21. M. KUWAHARA, H. SHIMOOKA, I. KATAYAMA and T. INADA, Preprints of 2nd Fall Meeting of Japanese Ceramics Society, Kyoto, 1989, p. 452.
22. X. PING and R. XU, *J. Mater. Sci. Lett.* **8** (1989) 1511.
23. A. ROSHKO, Y. M. CHIANG, J. S. MOODERA and D. A. RUDMAN, in "Superconductor II" (American Ceramic Society, 1989) p. 308.
24. T. YAMASHITA, A. KAWAKAMI, S. NOGE, W. XU, M. TAKATA, T. KOMATSU and K. MATSUSHITA, *Jpn. J. Appl. Phys.* **27** (1988) L1107.
25. H. MASUDA, F. MIZUNO, I. HIRABAYASHI and S. TANAKA, *ibid.* **28** (1989) L1226.
26. P. G. de GENNES, *Rev. Mod. Phys.* **36** (1964) 226.

Received 5 April
and accepted 20 December 1990